BLADE TYPE CAVITATION PREDICTION ON THE TWICE DEFORMATION OF AGRICULTURAL AUTOMOBILE ENGINE COOLING WATER PUMPS BASED ON CFD

/

基于 CFD 的农用汽车发动机冷却水泵二次变曲率叶型空化特性预测

Lect. Ph.D. Xue Dangqin[1, 2], Lect. Ph.D. Ma Shibang[3], Lect. Ph.D. Eng. Shi Huojie [4] , Prof. Ph.D. Hou Shulin[1]
[1] College of Engineering ,China Agricultural University, Beijing / China; [2] School of Mechanical ＆Automotive Engineering, Nanyang Institute of Technology, Henan / China;[3] Nangyang Normal University, Henan / China;
[4]Department of Biological Systems Engineering, Washington State University, Pullman / U.S.A.
Tel: +8613782173858; Email: xdq5599@163.com

Abstract: *Based on the CFD imitation of the three-dimensional flow field of the agricultural automobile engine cooling water pump, the thesis analyzes the energy characteristics and cavitation performance of the farm vehicle using two variable curvature blade type cooling water pump without cavitation, forecasts the cavitation distribution in the impeller and the stream line load distribution under different cavitation conditions and compares with the test results. The results showed that: in the design flow of 25 ℃, the simulated head was13.49m and the error between numerical simulation and the test results was within 2%. The head of the pump engine cooling model of agricultural vehicles of the design operating point under 85℃ is 9.6m, much lower than the head value of the design flow under 25℃. This shows that there is serious cavitation in the actual operation of pump, the cavitation performance curve and the numerical change trend converge, numerical value is less than the full cavitation range measured values and as the flow increases, the critical cavitation allowance also increases accordingly. The research provides a theoretical basis for the improvement of the cavitation performance of agricultural machinery engine cooling water pumps and the prevention and mitigation of cavitation.*

Keywords: *The two curvature blade; Cooling water pump of agricultural automobile engine; Cavitation performance; Leaf blade load; Performance prediction*

摘要： *基于 CFD 模拟农用汽车发动机冷却水泵内部的三维湍流流场，分析了某一农用汽车采用二次变曲率叶型冷却水泵无空化时的能量特性和空化性能，预测了不同空化状态下叶轮内的空泡分布和叶片中间流线上载荷分布，并与实验结果进行对比。结果表明：在 25℃设计流量下，模拟得到的扬程为 13.49m，数值模拟及试验的扬程和效率误差在 2%以内。在 85℃下农用汽车发动机冷却模型水泵在设计工况点的扬程为 9.6m，大大低于 25℃下设计流量下的扬程值。说明在实际运行时泵内已发生严重汽蚀，设计工况下的空化性能曲线与数值计算变化趋势一致，全空化范围内实测值小于数值计算值，而随着流量增大，临界汽蚀余量也相应增大。研究结果对于改善农用机械发动机冷却水泵的汽蚀性能、防止和减轻空化现象的产生提供了理论依据。*

关键词: *两段变曲率叶型; 农用汽车发动机冷却水泵; 空化性能; 叶片载荷; 性能预测*

INTRODUCTION

Cooling water pump of agricultural automobile engines is the key component to ensure the normal work of the engine cooling system and influences more of the performance of the engine. While cavitation has also influenced the performance of the cooling pump. The production and development of cavitation accompanied by the vibration, noise and even corrosion damage of flow parts, which will degrade the pump performance and shorten its service period [10]. Compared with common pumps, the cooling water pump, with high work temperature, large speed change range and limited size, is more prone to cavitation [7, 8]. The cavitation leads to the degradation of the performance and causes instability of the engine cooling system.

In view of the seriousness of the cavitation damage, both domestic and foreign scholars have conducted in-depth studies on cavitation of the inner mechanical flow field. R.F.Kunz and some researchers [4] predicted the occurrence and development of cavitation by applying two-phase flow model based on Navier-Stokes equation and obtained good effect; Luo Xianwu and some other researchers [10], based on VOF cavitation model numerical simulation on the whole flow field, conducted a systematical study on the influence of the impeller inlet parameter on

引言

农用汽车发动机冷却水泵是保障发动机冷却系统正常工作的关键部件，对发动机的性能影响日益显著。而空化现象对发动机冷却水泵的性能具有重要的影响，空化的产生、发展往往会伴随着产生振动、噪声甚至是过流部件的腐蚀破坏，降低泵的性能并缩短其服役期[10]。而在农用汽车发动机冷却系统中，由于冷却水泵具有工作温度高，转速变化范围大和结构尺寸总体受限等特殊性，其与普通水泵相比更容易发生空化现象[7,8]。空化现象造成的性能急降和空化破坏严重影响发动机冷却系统的稳定性。

鉴于空化破坏的严重性，国内外学者对机械内部流场的空化现象进行了深入研究。R.F.Kunz 等[4]对运用基于 Navier-Stokes 方程的两相流模型对空化的发生和发展进行了预测，获得了良好的效果；罗先武等[10]基于 VOF 空化模型对锅炉给水泵全流场进行数值模拟，系统地对叶轮进

cavitation and found that the low specific speed centrifugal pump in the direction of the wheel hub properly extending blade inlet edge and the use of blade placing angle can improve the cavitation performance of the pump; Wang Yong and some researchers [3,7,13], based on CFD technology numerical simulation of centrifugal pump, found that the cavitation performance under design conditions has no significant difference in different angles and analyses the cavitation distribution in the impeller and the stream line load distribution under different cavitation conditions.

The thesis studies a specific two curvature blade agricultural automobile engine cooling water pump which has appeared severe cavitation damage in the actual operation. By using CFD numerical simulation on the unsteady flow cavitation, it forecasts the location and the degree of cavitation damage and provides reference for the prediction of the impeller cavitation performance optimization and cavitation performance.

MATERIAL AND METHOD

The engine cooling water pump works under（85±2）°C in clear water, whose performance parameters and basic geometric parameters are shown in Table 1. Due to the special requirements of cylinder structure and agricultural vehicle engine, the design method of engine cooling water pump is different from the ordinary one, impeller width wide and impeller semi-open, the structure shown in figure 1, and the suction chamber section is annular. Use Creo 2 to generate the model pump whole field three-dimensional map, the computational domain shown in figure 2.

口参数对空化的影响进行了研究，发现对低比转速离心泵朝轮毂方向适当延伸叶片进口边，并采用较大的叶片安放角可以改善泵的空化性能；王勇等[3,7,13]基于 CFD 技术对离心泵进行数值模拟，发现不同叶片包角对设计工况下空化性能无明显影响，并分析了不同空化状态下叶轮中间截面内的空泡分布和叶片中间流向的载荷特性。

本文针对某一采用两段变曲率叶型的农用汽车发动机冷却水泵进行研究，其在实际运行中出现了较为严重的汽蚀破坏。利用 CFD 软件对其全流场的定常空化流动进行数值模拟，预测流道内空化发生的部位和程度，为叶轮空化性能的优化和空化性能的预测提供参考。

材料与方法

发动机冷却水泵工作条件为（85±2）℃温度条件下的清水介质，性能参数和基本几何参数如表 1 所示，由于缸体结构及农用汽车发动机的特殊要求，发动机冷却水泵的设计方法与普通的离心泵设计方法不一样，叶轮宽度较宽，叶轮为半开式，其结构型式如图 1，吸水室截面为环形。采用 Creo 2.0 生成了模型泵全流场三维立体图，计算域如图 2。

Table 1

Design and structure parameters of pump

parameters	values
flow/(kg·h-1)	8
head/m	14
rotation rate/(r·min-1)	3700
impellerouterdiameter/mm	53
impeller output width/mm	7
the number of blades	6

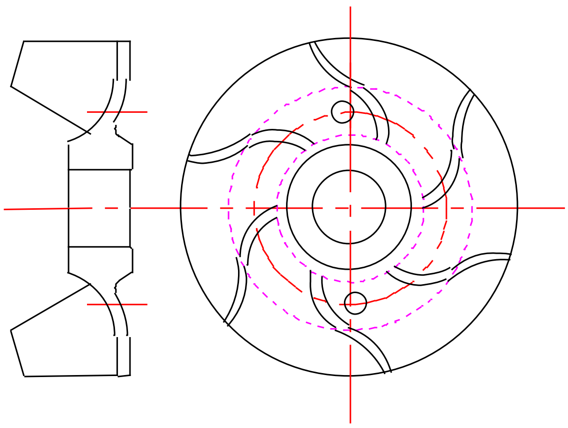

Fig.1 - The impeller's structure

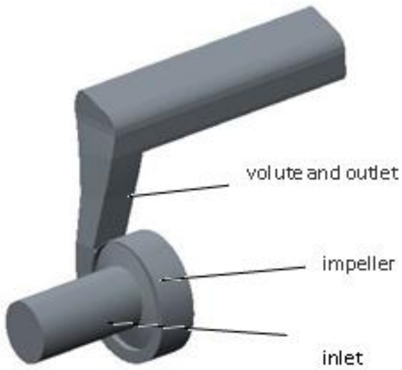

Fig.2 - The computational domain three-dimensional map

The choice of numerical model

In single phase calculation, take N-S equations as governing equations and Standard *k-ε* turbulence model as 3D turbulent numerical calculation. The turbulent kinetic energy *k* and the dissipation rate of turbulent kinetic energy *ε* of turbulent transport equation model is:

数值模型的选择

单相计算以时均 N-S 方程作为基本控制方程，利用 Standard k-ε 湍流模型进行三维湍流数值计算。该湍流模型湍动能 k 和湍动能耗散率 ε 的输送方程为:

$$\mu_t = \rho C_\mu \frac{k^2}{e} \tag{1}$$

$$\frac{\partial(\rho k)}{\partial t} + \frac{\partial(\rho k u_i)}{\partial x_i} = \frac{\partial}{\partial x_j}\left[\left(\mu + \frac{\mu_t}{\sigma_k}\right)\frac{\partial e}{\partial x_j}\right] + G_k - \rho e \tag{2}$$

$$\frac{\partial(\rho e)}{\partial t} + \frac{\partial(\rho e u_i)}{\partial x_i} = \frac{\partial}{\partial x_j}\left[\left(\mu_\varepsilon + \frac{\mu}{\sigma_\varepsilon}\right)\frac{\partial e}{\partial x_j}\right] + \frac{C_{1\varepsilon}}{k} G_k - C_{2\varepsilon}\frac{\rho e^2}{k} \tag{3}$$

Where: μ_t - the turbulent kinematic viscosity;
G_k - the generation item of mean velocity gradient caused by the turbulent kinetic energy *k;*
σ_k - the prandtl number corresponding to turbulent kinetic energy *k*; σ_k=1.0;
σ_ε - the prandtl number corresponding to dissipation rate epsilon; σ_ε=1.3;
C_μ , $C_{1\varepsilon}$ and $C_{2\varepsilon}$ are empirical constant, C_μ=0.09; $C_{1\varepsilon}$=1.44; $C_{2\varepsilon}$=1.92.

In this thesis, multi-phase simulation uses flow field and velocity field of same Homogeneous Model and vapor - liquid two - phase. Cavitation is calculated by Rayleigh-Plesset model which provides rate equations and condensing vacuoles produced. The development process of the bubble in the fluid is as below:

式中：μ_t - 湍流运动粘度
G_k - 平均速度梯度引起的湍动能 k 的产生项
σ_k - 湍动能 k 对应的 Prandtl 数；σ_k=1.0
σ_ε - 耗散率 ε 对应的 Prandtl 数；σ_ε=1.3
C_μ，$C_{1\varepsilon}$ 和 $C_{2\varepsilon}$ 为经验常数，C_μ =0.09；$C_{1\varepsilon}$=1.44；$C_{2\varepsilon}$=1.92.

本文的多相模拟采用 Homogeneous Model 及汽液两相具有相同的流场和速度场。空化计算采用 Rayleigh-Plesset 模型，该模型给出了空泡产生和凝结的速率方程，汽泡在流体中的发展过程如下式:

$$R_B \frac{d^2 R_B}{dt^2} + \frac{3}{2}\left(\frac{dR_B}{dt}\right)^2 + \frac{2\sigma}{\rho_f R_B} = \frac{p_v - p}{\rho_f} \tag{4}$$

Where, R_B—the bubble radius
p_v—the inside cavity pressure
p—the around bubble pressure of fluid
ρ_f—fluid density
σ—the coefficient of surface tension and bubble

Note that the equation (4) does not consider the influence of thermal effects on the development of cavitation. Ignoring the order condition and surface tension, equation (4) is simplified as:

式中：R_B——汽泡半径
p_v——空泡内的压力
p——空泡周围流体的压力
ρ_f——流体密度
σ——流体与空泡交界面的表面张力系数

要注意的是方程（4）未考虑热效应对空泡发展的影响。在忽略二阶条件和表面张力的条件下，方程（4）简化为:

$$\frac{dR_B}{dt} = \sqrt{\frac{2}{3}\frac{p_v - p}{\rho_f}} \tag{5}$$

The change rate of the vacuole volume:

则空泡体积的变化速率：

$$\frac{dR_B}{dt} = \frac{d}{dt}\left(\frac{4}{3}\pi R_B^3\right) = 4\pi R_B^3 \sqrt{\frac{2}{3}\frac{p_v - p}{\rho_f}} \tag{6}$$

the quality change rate of the vacuole:

空泡的质量变化速率：

$$\frac{dm_B}{dt} = \rho_g \frac{dV_B}{dt} = 4\pi R_B^2 \rho_g \sqrt{\frac{2}{3}\frac{p_v - p}{\rho_f}} \tag{7}$$

If there are N_B vacuoles per unit volume, the volume fraction of r_g can be expressed as:

如果在每单位体积内有 N_B 个空泡，则其体积分数 r_g 可以表示为:

$$r_g = V_B N_B = \frac{4}{3}\pi R_B^3 N_B \tag{8}$$

The transfer rate of overall mass of unit volume:

单位体积内总体相间质量传输速率为：

$$\dot{m}_{fg} = N_B \frac{dm_B}{dt} = \frac{3r_g\rho_g}{R_B}\sqrt{\frac{2}{3}\frac{p_v - p}{\rho_f}} \tag{9}$$

The equation is derived by the development of the vacuoles (vaporization). When taking the bubble condensation into consideration:

上式由空泡的发展（汽化作用）推导得到。

在考虑空泡凝结作用时，得到：

$$\dot{m}_{fg} = F\frac{3r_g\rho_g}{R_B}\sqrt{\frac{2}{3}\frac{|p_v - p|}{\rho_f}}\operatorname{sgn}(p_v - p) \tag{10}$$

Although the equation can be commonly used in the vaporization and condensation process, it should be further optimized in vaporization. Vaporization starts at nucleation. With the increase of vacuole volume fraction, the nucleation density must decreases accordingly. r_{nuc} (1-r_g) taking place of r_g:

尽管上式普遍使用与汽化和凝结过程，在汽化情况下仍需要进一步的优化。汽化作用起始于成核位置，随着空泡体积分数的增长，成核中心密度必然相应下降。用 r_{nuc}（1-r_g）代替上式中的 r_g:

$$\dot{m}_{fg} = F\frac{3r_{nuc}(1-r_g)\rho_g}{R_B}\sqrt{\frac{2}{3}\frac{|p_v - p|}{\rho_f}}\operatorname{sgn}(p_v - p) \tag{11}$$

Where, F - empirical coefficient

r_{nuc} - nucleation position volume fraction

R_B - The nucleation semi-diameter is gained through documents. 85℃ saturated main steam parameters is shown in table 2.

式中:F - 经验系数

r_{nuc} - 成核位置体积分数

R_B - 此式中指成核位置的半经由文献得到 85℃下饱和水蒸汽的主要物性参数，如表 2。

Table 2

85°C saturated main steam parameters

Material Properties	Value
Thermodynamic state	Gas
Molar Mass/kg·kmol^{-1}	18
Density/kg·m^{-3}	0.35735
Specific heat capacity/J·g^{-1}·K^{-1}	1.88
Specific heat type	Constant pressure
Dynamic viscosity/Pa·s	346.8
Thermal conductivity/W·m^{-1}·K^{-1}	695.6
Saturation pressure/kPa	57.815

Mesh generation and boundary condition

ICEM hexahedral mesh generation is applied to the model pump full flow field and 10-15 layer to the big part of the impeller radius of curvature to ensure the block accord with the internal flow of the agricultural machinery engine cooling pumps while ensuring the calculation accuracy of the impeller near wall [6]. In order to obtain the most economical grid number and calculation step, the independent mesh study on numerical simulation under the design condition is conducted. It shows that when the number of the mesh reaches above 1,500,000, the change range of the head is within 2%, which can think as mesh having no influence on the calculation results. Impeller block and the computational domain mesh are shown in Figure 3.

网格划分和边界条件

对模型泵全流场采用 ICEM 进行六面体网格划分，对叶轮曲率半径较大的地方设置 10-15 层的边界层网格，在保证分块较好符合农用机械发动机冷却泵内的流动状态的同时保证叶轮近壁面的计算精度[6]。为了获得最经济的网格数和计算步长，对设计工况下的数值模拟进行了网格无关性的研究，发现当网格数达到 150 万以上时，扬程的变化幅度在 2%之内，可以认为网格对计算结果没有影响。叶轮的分块及计算域网格如图 3。

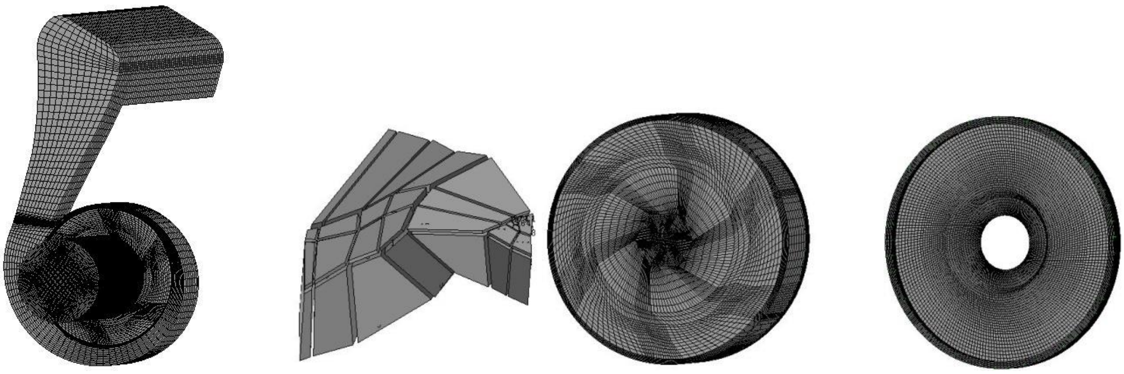

(a) Full flow field mesh model (b) Impeller block and mesh model (c) The impeller back cavity mesh model

Fig. 3 - The computational domain mesh

The cavitation allowance (NPSH) is closely related to the inlet pressure of the pump, and therefore the boundary conditions of the pressure inlet and mass flow outlet are applied to the model pump. Inlet bubble phase volume fraction is set to 0, the volume fraction of liquid phase 1 and the surface roughness 0.02mm; the near wall uses standard wall function, the wall boundary condition is set to no slip insulation wall [2].

Cavitation simulation takes the no-cavitation calculation results as the initial results. By changing the inlet pressure, the centrifugal pump cavitation occurs and then obtains better calculation convergence effect, so as to shorten the time of calculation [12].

由于空化余量（NPSH）与泵的进口压力密切相关，因此对模型泵采用压力进口和质量流量出口的边界条件。设置进口空泡相体积分数为 0，液相体积分数设为 1。壁面粗糙度设为 0.02mm；近壁面处选用标准壁面函数，壁面边界条件设为绝热无滑移壁面[2]。

空化模拟计算以无空化计算结果作为计算的初始结果。通过改变进口压力使离心泵发生空化，这样能获得较好的计算收敛效果，从而缩短计算时间[12]。

RESULTS

Validation and comparison between the external characteristics numerical simulation results and the experimental results

For the cavitation free single-phase flow, the flow – head and flow - efficiency curve under 25℃ is calculated under the five conditions of 0.7 Q_d, 0.85 Q_d, 1.0 Q_d, 1.15 Q_d and 1.3 Q_d**.** From figure 4, the numerical simulation results agree well with the experimental results. In the 1.0 Q_d**,** the numerical simulation head is 13.49m and efficiency of 56.9%. As seen from the graph, under the five conditions selected, the efficiency has a high degree of goodness of fit. While the efficiency values obtained from the numerical calculation are higher than that of the experimental results, the error value within about 2% due to the ignoring of the mechanical loss caused by caused by the bearing and friction in numerical simulation process [1].

结果

外特性数值模拟结果与实验结果的对比验证

对于无空化单相流动时，在 25℃下分别在 0.7Q_d、0.85Q_d、1.0Q_d、1.15Q_d、1.3Q_d 五种工况下模拟计算出其流量-扬程和流量-效率曲线，从图 4 可以看出数值模拟得到的结果与实验结果吻合较好。此时在 1.0Q_d 数值模拟得到扬程为 13.49m，效率为 56.9%。从图中可以看出，所选取的五个工况中，效率吻合度较高，而数值计算得到的效率值均高于试验结果，误差值约在 2%左右，这是由于在数值模拟中忽略了轴承、摩擦副等引起的机械损失[1]。

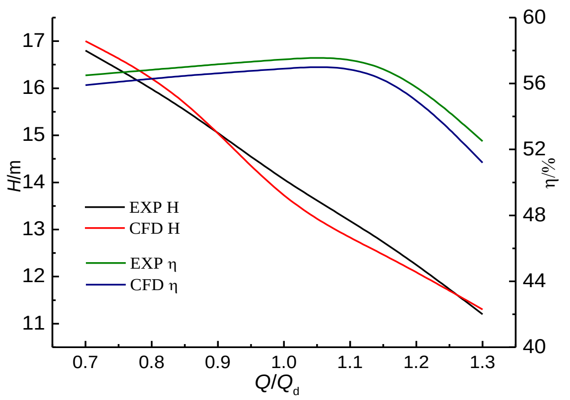

Fig. 4 - 25℃ model pump numerical simulation and experimental

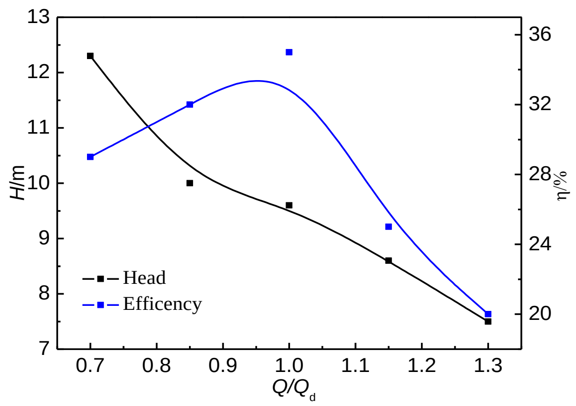

Fig. 5 - 85℃ performance curve of the model pump

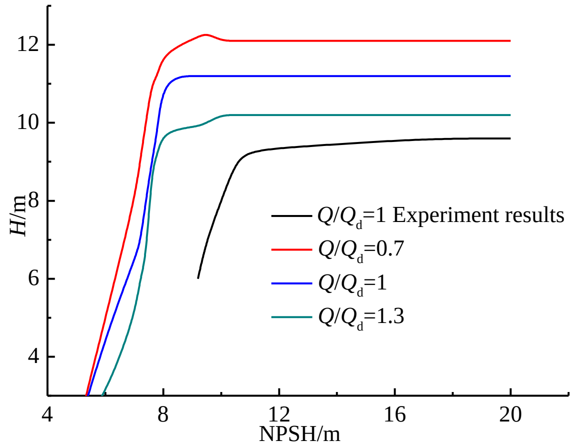

Fig. 6 - Comparison of calculated value and cavitation test

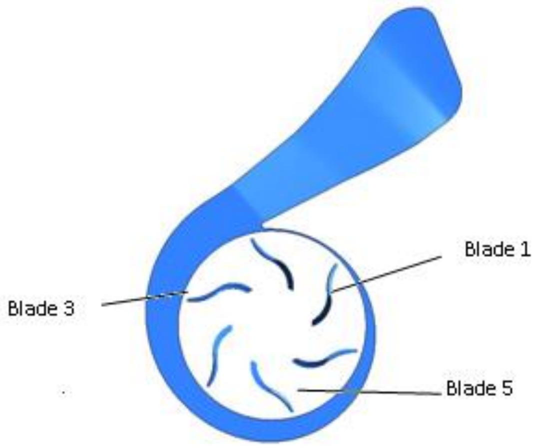

Fig. 7 - The blade numbers

In the outer characteristic test, when heated to about 85℃, the head is 9.6m of the model pump under the design flow head. At the same time, the gradual change of the net energy absorbing head [5] occurs when keeping a constant flow, changing the inlet opening and reducing the pump inlet pressure by increasing the inlet resistance. When the head drops 3%, the NPSH (NPSH) is 11m. Test characteristic curve obtained under 85℃ is shown in figure 5, and the cavitation performance curve of the model pump under the design condition and the simulation results of $0.7Q_d$, 1.0 Q_d and 1.3 Q_d under the condition are shown in figure 6.

Seen from the figure, the overall decline in the performance of the model pump at the temperature of 85℃ is greater than that under the temperature of 25℃. From figure 6, the cavitation performance curve and numerical calculation change are prone to be the same under the design condition, the measured numerical value within the full cavitation range is less than the calculated value; when the flow rate increases, the critical cavitation allowance also increases accordingly; in each case, when NPSH>11.5m, the increasing of NPSH has little effect on the head.

The load distribution on the blade surface

The blade surface load is the difference between the pressure surface and the suction surface of a same blade, which is an important parameter affecting the cavitation performance. If the pressure difference defined, it is:

在外特性试验中，当加温至 85℃左右，模型泵在设计流量扬程下扬程为 9.6m，同时进行汽蚀性能试验，保持流量不变，改变进口阀门的开度，通过增加进口阻力来降低模型泵进口压力，从而逐渐改变净吸能头[5]。当扬程下降 3%时，得到汽蚀余量（NPSH）为 11m。在 85℃温度下得到的试验外特性曲线如图 5，而模型泵在设计工况的空化性能曲线与 $0.7Q_d$、$1.0Q_d$ 及 $1.3Q_d$ 工况下模拟结果如图 6。

可以发现，85℃下模型泵的整体性能比在 25℃下有极大的下降。由图 6 中可以看出，设计工况下的空化性能曲线与数值计算的变化趋势一致，全空化范围内实测值小于数值计算值，而随着流量增大，临界汽蚀余量也相应增大；在各工况下，当 NPSH>11.5m 时，汽蚀余量的增大对扬程几乎没有影响。

叶片表面载荷分布

叶片表面载荷是同一叶片和相同半径处压力面和吸力面压力之差。而叶片两面的压力差是影响空化性能的重要参数。将这一压力差量纲化，即：

$$\Delta p=\frac{p_{ps}-p_{ss}}{\frac{1}{2}\rho U^2} \tag{12}$$

Where: p_{ps} - the middle streamline pressure of the pressure surface

p_{ss} - the middle streamline pressure of the suction surface

U - The circular velocity blade numbers used at the intersection of the impeller blade inlet edge and the front cover plate are shown in figure 7. Figure 8 is about the load distribution curve of the blade surface and the middle streamline of the pump model under the design flow, the abscissa shows the relative position of a point on the streamline.

式中：p_{ps} - 压力面表面中间流线压强

p_{ss} - 吸力面表面中间流线压强

U - 模型泵中采用叶轮叶片进口边与前盖板交点处的圆周速度叶片序号如图 7，图 8 为模型泵在设计流量下各叶片表面的叶片中间流线上载荷分布曲线，其中横坐标表示某点在流线方向上的相对位置。

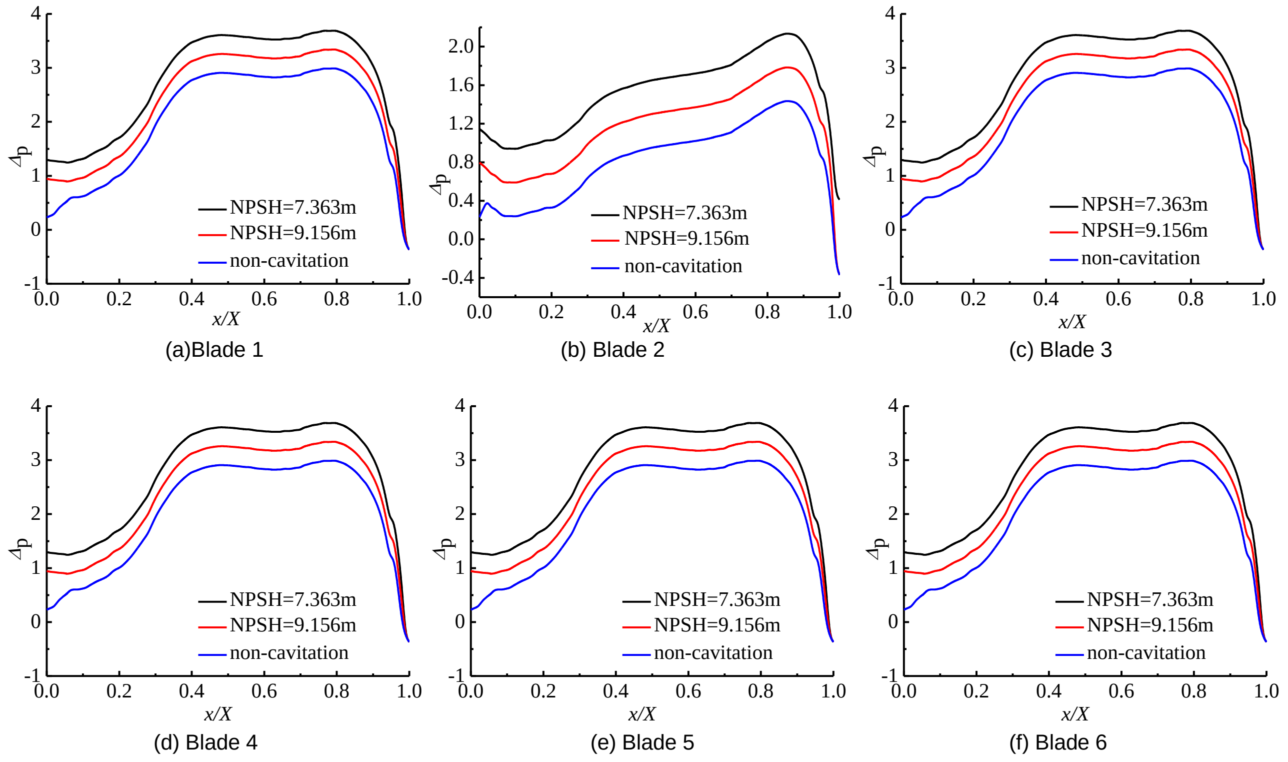

Fig. 8 - The load distribution curve of the blade middle streamlines

It can be seen from the figure 8 that from the blade inlet to outlet, except for blade 2, the curve appears an parabolic increasing; when x/X=0.5~0.8, the pressure difference coefficient appears a stable trend and the fluid enters the bended part of the two curvature blade impeller; when x/X > 0.8, the nearer impeller outlet, its pressure difference steeply drops, which may even lead to the pressure of the suction surface exceeding that of the pressure surface. This is because near the outlet, the fluid flows into the suction surface from the working surface, during which leakage happens and results in decreased pressure difference coefficient. While at the inlet of the blade 2, the pressure coefficient is higher than that of the other 5 blades, but the overall pressure difference coefficient is small so that the load on blade 2 is minimum. Comparing the different NPSH coefficient of the pressure difference, it find that as the NPSH decreases, the pressure difference coefficient rise of all the blades, which shows that cavitation has great influence on blade loading and the blade pressure difference coefficient is in direct proportion to cavitation.

Inner impeller cavitation bubbles distribution

According to the saturated vapor pressure hypothesis, when the inner pressure of the pump is lower than the medium corresponding operating pressure, cavitation bubble will happens to the fluid medium. Figure 9 shows the void distribution under different NPSH in the impeller. We can see from Figure 4, as the NPSH decreases, the inside pump cavitation volume distribution increases. Vacuoles appear first at the blade inlet edge near the back flow passage and near the baffle tongue with an asymmetric distribution. Inside the pump the vacuole volume increases as the NPSH decreases, along the blade impeller back to drain diffusion, and extends to the pressure surface. When NPSH=7.363m, it can be found that the cavitation bubbles have occupied much of the channel, greatly influencing the performance of the

由图 8 可以看出从叶片进口到出口，除叶片 2 外基本呈抛物线形趋势增加；当 x/X=0.5~0.8 时，压差系数出现平稳趋势，此时流体进入二段变曲率叶型叶轮的后弯部分；当 x/X 大于 0.8 时，及靠近叶轮出口处，压差陡降，甚至吸力面的压力会超过压力面，这是由于在出口边处，流体由工作面流入吸力面，产生泄漏流，造成压差系数的下降。而叶片 2 在叶片入口处，压力系数高于其他 5 个叶片，但是总体上压差系数较小，叶片 2 上所受载荷也就最小。对比不同 NPSH 时的压差系数，发现随着 NPSH 的减小，在各叶片上的压差系数都呈明显的上升，说明空化对于叶片载荷有较大的影响。同时也说明叶片压差系数越高，空化越严重。

叶轮内部空泡分布

根据饱和蒸汽压的假说，当泵内的压力小于介质相应工况的饱和蒸汽压时，流体介质将发生汽化产生空泡。图 9 为不同 NPSH 下叶轮内的空泡分布。由图 4 可知，随着 NPSH 的减小，泵内部的空泡体积分布增大，空泡首先在叶片背面进口边附近出现，并且首先出现在靠近隔舌的流道内，且在全流量内空泡的分布成不对称分布。泵内部的空泡体积随着 NPSH 的减小而增大，沿叶片背面向叶轮处漏扩散，并同时向压力面方向扩展。在 NPSH=7.363m 时，可以发现，空泡已经占据了很大部分的流道，极大地影响了泵的性能。在同一 NPSH 下， 空化程度随着流量

pump. In the same NPSH, the cavitation becomes serious as the flow rate increases. Figure10 shows the vacuole distribution of the 1.0Q_d impeller intermediate flow and reflects the distribution rule. When NPSH=10.541m, there's no void distribution in the intermediate flow, cavitation is mainly distributed at the inlet near the front pump cavity edge; as the decline of NPSH to 7.363m, the flow near the baffle tongue is almost blocked by the vacuoles, where there appears obvious fault in the external characteristics.

Figure 11 shows the static pressure distribution the middle section of the impeller 1.0Q_d cases. As seen from the graph, when the NPSH=10.541m, at the cavitation inception stage, there's no void distribution in the middle section but obviously appears in the low pressure area. With the decline of HPSH, near the septal area of low pressure in the flow channel near the tongue first appear the attachment holes which make the water flow channel separated from the solid boundary. When HPSH=9.156m, we can see that the vacuoles cross the channels and cavitation bubbles appear in each channel. Except for the channel near the separation tongue, the static pressure in the flow passage appears a symmetrical distribution.

增大而变得严重。图 10 为 1.0Qd 叶轮中间流面内空泡分布,也体现了上述的分布规律。NPSH=10.541m 时，在中间流面内无空泡分布，空泡主要分布在靠近前泵腔的进口边处，随着 NPSH 的下降，到 NPSH=7.363m 时，靠近隔舌的流道几乎被空泡堵塞，此时在外特性上出现明显的断裂。

图 11 为 1.0Q_d工况下叶轮中间截面上的静压分布，从图中可以看出，在 NPSH=10.541m 时，空化初生阶段，虽然在中间截面上无空泡分布，但是已存在明显的低压区，随着 HPSH 的下降，在靠近隔舌附近的流道内的低压区域首先发展为附着空穴，使水流从过流通道的固体边界脱离。在 HPSH=9.156m 时，可以看出空泡跨流道延伸，在各流道内均出现空泡，除靠近隔舌位置的流道，其他流道内的静压基本成对称分布。

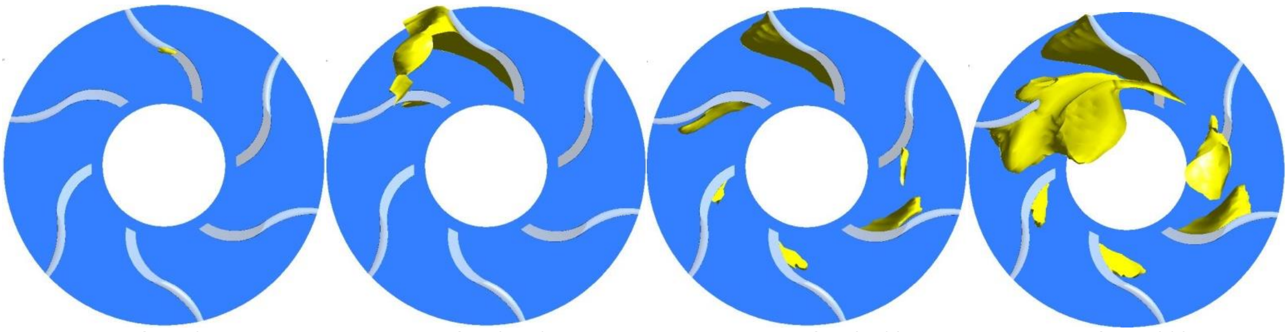

NPSH=10.541m HPSH=9.156m NPSH=8.163m NPSH=7.363m

(a) Q/Qd=0.7

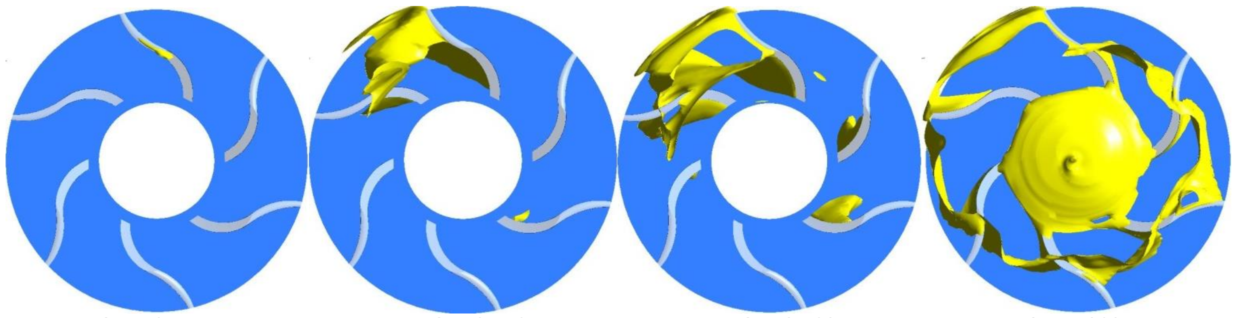

NPSH=10.541m HPSH=9.156m NPSH=8.163m NPSH=7.363m

(b) Q/Qd =1.0

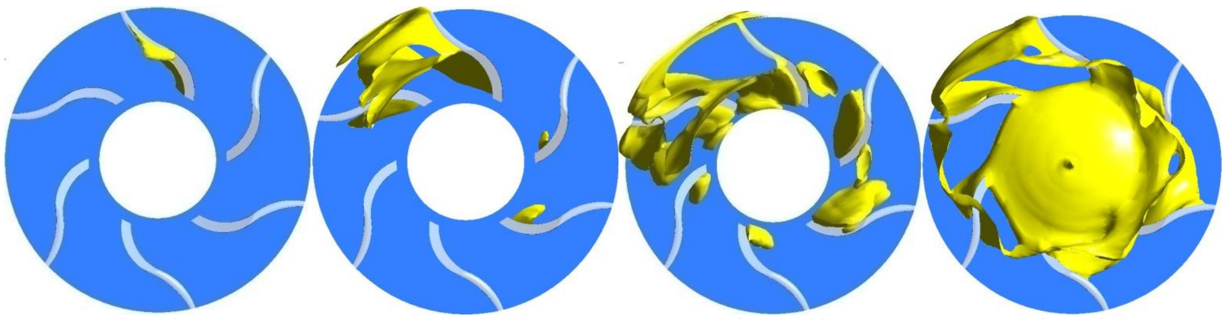

NPSH=10.541m HPSH=9.156m NPSH=8.163m NPSH=7.363m

(c) Q/Qd =1.3

Fig. 9 - Inner impeller cavitation bubbles distribution

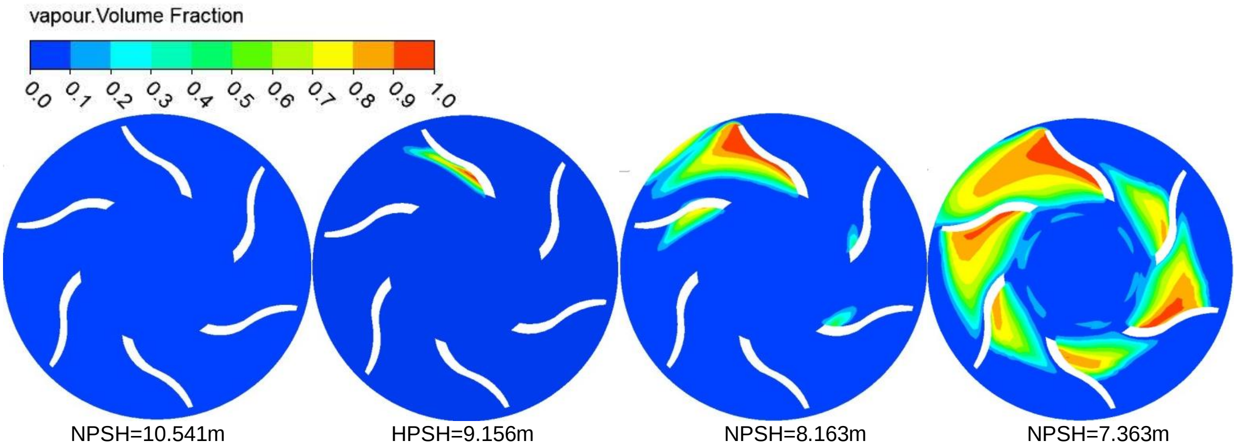

Fig. 10 - The void distribution in the intermediate flow surface of the impeller

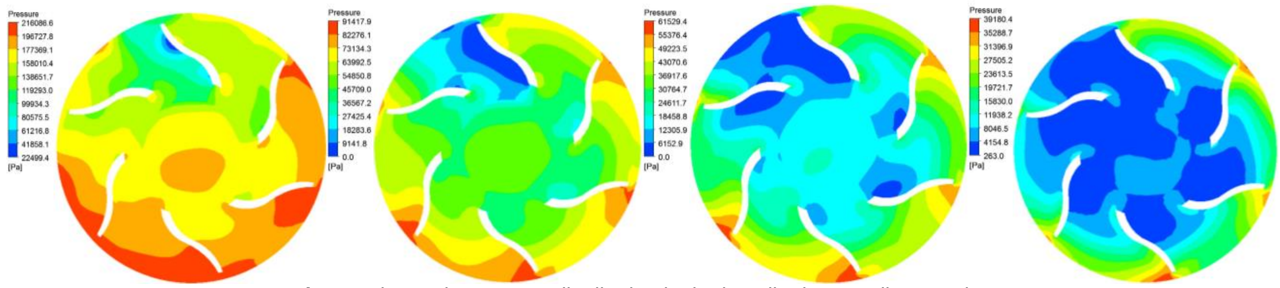

Fig.11- The static pressure distribution in the impeller intermediate section

CONCLUSIONS

(1) This thesis, adopting numerical calculating method, studies that the cavitation performance curve and the calculation values are prone to be same, the numerical calculation value is lower than the measured value in the full cavitation range, and will provide a good guiding for the agricultural and fluid pump application.

(2) For the blades near the baffle tongue, regardless of pump cavitation or not, the pressure difference coefficient on the streamlines is minimum. With the development of cavitation, the pressure difference coefficient on the middle streamline increases obviously, which proves that the cavitation has a significant influence on the load of the blades.

(3) For the two curvature blade type centrifugal pump, as the inlet pressure decreases, cavitation bubbles occur firstly at the blade inlet and then extend to the impeller outlet along the streamline, until there appear a large number of cavitation bubbles on the pressure surface of blade curved part.

ACKNOWLEDGEMENT

The study was supported by the National High technology and Development Program of china (2012AA10A503), Science and Technology Research Project of Henan Province (142102210555).

REFERENCES

[1]. Fan Yang, Chao Liu, (2013) - *Numerical and Experimental Investigation of Slanted Axial-flow pumping System,* Journal of Engineering Science and Technology Review, vol.6，no.2, pp.62-68;

[2]. Halima Hadziahmetovic, Nedim Hodzic, Damir Kahrimanovic, Ejub Dzaferovic, (2014) - *Computational fluid dynamics (CFD) based Erosion Prediction Model in Elbows,* Technical Gazette, vol.21, no.2, pp. 275-282;

结论

（1）本文中采用的数值计算方法，空化性能曲线与数值计算变化趋势一致，全空化范围内实测值小于数值计算值，对农业及流体泵类应用具有较好的指导意义。

（2）在靠近隔舌的叶片上，无论水泵是否出现空化现象，其中间流线上，压差系数最小。随着空化的发展，叶轮中间流线的压差系数明显增大，说明空化对叶片的载荷有重要影响。

（3）对于二次变曲率叶型离心泵，随着进口压力的降低，空泡首先出现在叶片进口处，然后沿流线向叶轮出口扩展，直至在叶片后弯部分的压力面出现大量空泡。

致谢

国家高技术研究发展计划（2012AA10A503），河南省科技攻关项目资助（142102210555）

参考文献

[1]. 杨帆, 刘超, (2013) - *斜式轴流泵系统的数值模拟和实验研究*,工程科学与技术杂志,第 6 卷,第 2 期, 62-68;

[2]. Halima Hadziahmetovic, Nedim Hodzic, Damir Kahrimanovic, Ejub Dzaferovic, (2014) -*基于计算流体动力学(CFD)的肘部流失模型预测*,科技公报,第 21 卷,第 2 期, 275-282;

[3]. Houlin Liu, Dongxi Liu,Yong Wang, (2012) - *Applicative Evaluation of Three Cavitating Models on Cavitating Flow Calculation in Centrifugal Pump,* Transactions of the CSAE, vol. 28, no. 16, pp.54-59;
[4]. Kunz R.F., Boger D.A., Stinebring D.R., (2000) - *A preconditioned Navier–Stokes method for two-phase flows with application to cavitation prediction*, Computers & Fluids, vol. 39, no.4, pp. 849-875.
[5]. Lei Tan, Shuliang Cao, Shaobo Gui, (2010) - *Experiment and Numerical Simulation of Cavitation Performance for Centrifugal Pump with Inlet Guide Vane,* Journal of Mechanical Engineering, vol. 46, no 18, pp.177-182;
[6]. Weidong Cao, Xiaodi Zhang, Yi Gao, (2012) - *Cavitation Performance of the Low Specific-speed Centrifugal Pump with Radial Reflux Balance Hole,* Transactions of the Chinese Society for Agricultural Machinery, vol. 43, no 1, pp.37-41;
[7]. Yong Wang, Houlin Liu, Shouqi Yuan, (2012) - *Experimental Testing on Cavitation Vibration and Noise of Centrifugal Pumps under off-design Conditions,* Transactions of the CSAE, vol. 28, no.2, pp.35-38;
[8]. Wei Li, Weidong Shi, Bing Pei, (2013) - *Numerical Simulation and Improvement on Cavitation Performance of Engine Cooling Water Pump,* Transactions of CSICE. vol. 31, no.2, pp.165-170;
[9]. Wei Li, Weidong Shi, Hua Zhang, (2012) - *Cavitation Performance Prediction of Engine Cooling Water Pump based on CFD,* Journal of Drainage and Irrigation Machinery Engineering, vol. 30, no.2, pp.176-180;
[10]. Xianwu Luo, Yao Zhang, Junqi Peng, (2008) - *Effect of Impeller inlet Geometry on Centrifugal Pump Cavitation Performance,* J Tsinghua (Sci & Tech), vol. 48, no.5, pp.836-839;
[11]. Xingfan Guan, (1987) –*Theory and Design of Pump,* Beijing: China Machine Press;
[12]. Yongsheng Su, Yongsheng Wang, Xiangyang Duan, (2010) - *Cavitation Experimental Research on Centrifugal Pump,* Transactions of the Chinese Society for Agricultural Machinery, vol. 41, no 3, pp.77-80;
[13]. Yong Wang, Houlin Liu, Shouqi Yuan, (2011) -*CFD Simulation on Cavitation Characteristics in Centrifugal Pump,* Journal of Drainage and Irrigation Machinery Engineering, vol. 29, no.2, pp.99-103.

[3]. 刘厚林, 刘东喜, 王勇, 等.(2012) - *三种空化模型在离心泵空化流计算中的应用评价*, 农业工程学报, 第 28 卷, 第 16 期, 54-59;
[4]. Kunz R.F., Boger D.A., Stinebring D.R.,（2000）- *基于 Navier–Stokes 方程的两相流模型空化预测*,.计算流体，第 29 卷, 第 8 期, 849-875;
[5]. 谭磊, 曹树良, 桂绍波, 等, (2012) - *带有前置导叶离心泵空化性能的试验及数值模拟*, 机械工程学报, 第 46 卷, 第 18 期, 77-80;
[6]. 曹卫东, 张晓娣, 高一, 等 (2012) - *径向回流平衡孔低比转数离心泵空化性能研究,* 农业机械学报, 第 43 卷, 第 1 期, 37-41;
[7]. 王勇, 刘厚林, 袁寿其, 等 (2012) - *离心泵非设计工况空化振动噪声的试验测试,* 农业工程学报, 第 28 卷, 第 2 期, 35-38;
[8]. 李伟,施卫东,裴冰,等 (2013) - *发动机冷却水泵空化特性的数值模拟与改进,* 内燃机学报, 第 31 卷, 第 2 期, 165-170;
[9]. 李伟, 施卫东, 张华,等.(2012)- *基于 CFD 的发动机冷却水泵汽蚀性能预测,* 排灌机械工程学报, 第 30 卷, 第 2 期, 176-180;
[10]. 罗先武, 张瑶, 彭俊奇,等.(2008) - *叶轮进口几何参数对离心泵空化性能的影响,* 清华大学学报(自然科学版), 第 48 卷, 第 5 期, 836-839;
[11]. 关醒凡.(1987) - *泵的理论与设计*;北京:机械工业出版社;
[12]. 苏永生, 王永生, 段向阳 (2010) - *离心泵空化试验研究,* 农业机械学报, 第 41 卷, 第 3 期, 77-80;
[13]. 王勇, 刘厚林, 袁寿其, 等 (2011) - *离心泵内部空化特性的 CFD 模拟,* 排灌机械工程学报, 第 29 卷, 第 2 期, 99-103.